

Effect of disorder on charge-density wave and superconducting order in the half-filled attractive Hubbard model

C. Huscroft and R. T. Scalettar

Physics Department, University of California, Davis, California 95616

(Received 5 June 1996)

The half-filled attractive Hubbard model exhibits a simultaneous charge-density wave and superconducting order in its ground state. In this paper we use approximation-free quantum Monte Carlo techniques to explore the effect of disorder in the site energies on this degeneracy. We find that superconducting order survives randomness out to a critical amount of disorder, but charge ordering is immediately destroyed. This settles the issue as to whether disordered site energies, which do not break time-reversal invariance, can destroy pairing correlations. We also locate the precise ratio of disorder to bandwidth required for the disorder-driven transition from the superconducting state. We explore the validity of a strong-coupling picture which maps the system onto a Heisenberg model in a random magnetic field. [S0163-1829(97)05701-9]

I. INTRODUCTION

The repulsive Hubbard model has long served as a simple Hamiltonian to describe itinerant magnetism. Similarly, the attractive Hubbard model has been used to explore qualitative features of the superconducting phase transition.^{1,2} This model does not provide a microscopic model of the origin of pairing. Rather it is assumed that some other degrees of freedom, for example, an electron-phonon coupling, have already provided the necessary attraction. Recent quantum simulation studies³⁻⁸ have explored a number of features of the attractive Hubbard Hamiltonian, including a determination of the superconducting transition temperature and its dependence on electron density,⁹ the detailed spatial structure of the pairing correlations,¹⁰ the coexistence of a Bose-like spin gap with an otherwise degenerate Fermi gas of electrons,¹¹ and deviations from Fermi-liquid behavior.¹² Much analytic work has also been done, as reviewed in Ref. 2.

While the interplay of superconductivity and disorder has of course been extensively studied theoretically,¹³ considerably less is known numerically. The competition between the dephasing effect of impurity scattering and the dramatic manifestation of phase coherence in the zero-resistance state gives rise to a set of challenging qualitative questions. A quantitative understanding is also essential in order to model experiments like those which address the question of the possibility of a universal resistance in disordered superconducting films.¹⁴

Much recent theoretical^{15,16} and numerical¹⁷⁻²¹ work on these issues has been done within the context of the "boson-Hubbard" model; that is, under the assumption that preformed Cooper pairs exist even in the nonsuperconducting state, and that the transition is driven by the loss of phase coherence, rather than the destruction of the magnitude of the superconducting gap. This bosonic model should be the limit of the attractive Hubbard Hamiltonian as the on-site interaction U becomes large. Despite the greater computational simplicity of the boson models, it is the fermion system which is of fundamental interest.

In this paper we will explore the effect of random site energies in the attractive Hubbard Hamiltonian

$$H = -t \sum_{\langle i,j \rangle \sigma} (c_{i\sigma}^\dagger c_{j\sigma} + c_{j\sigma}^\dagger c_{i\sigma}) - |U| \sum_{\mathbf{i}} (n_{i\uparrow} - \frac{1}{2})(n_{i\downarrow} - \frac{1}{2}) + \sum_{\mathbf{i}} (\epsilon_{\mathbf{i}} - \mu)(n_{i\uparrow} + n_{i\downarrow}). \quad (1)$$

Here $c_{i\sigma}$ ($c_{i\sigma}^\dagger$) are operators which destroy (create) electrons of spin σ on site \mathbf{i} , so the first term in H describes the hopping of electrons between nearest-neighbor sites on our $2d$ square lattice. $|U|$ is the on-site attraction, while μ and $\epsilon_{\mathbf{i}}$ are the chemical potential and random site energies, respectively. $\epsilon_{\mathbf{i}}$ are chosen uniformly on $[-V, +V]$. In this paper, we will work exclusively at half-filling, $\langle n_{i\uparrow} + n_{i\downarrow} \rangle = 1$. A related study of the current-current correlations and the behavior of the resistivity as a function of disorder strength and temperature away from half-filling is contained in Ref. 22.

In the absence of disorder, $V=0$, considerable insight can be gained by considering the effect of a particle-hole transformation on the down-electron operators, $c_{i\uparrow} \leftrightarrow c_{i\uparrow}$, $c_{i\downarrow} \leftrightarrow c_{i\downarrow}^\dagger (-1)^{i_x+i_y}$. The phase factor $(-1)^{i_x+i_y}$ changes sign as one goes between the two sublattices of our (bipartite) square lattice. Under this transformation the kinetic energy is invariant, while the interaction changes sign, $|U| \leftrightarrow -|U|$. The chemical potential now couples to the z component of the spin on each site, instead of to the charge. In the absence of a chemical potential term, we have an exact mapping between the attractive and repulsive Hubbard Hamiltonians. Pair correlations in the attractive model map onto spin correlations in the xy plane of the repulsive model, while charge-density-wave (cdw) correlations are associated with spin correlations in the z direction. Since the long-range spin order in the ground state of the two-dimensional (2D) repulsive Hubbard model is rotationally invariant, we immediately conclude that pairing and cdw correlations coexist in the ground state of the half-filled attractive model. This mapping can also be used to discuss the effect of doping, as will be described in Sec. V.

In this paper we consider nonzero disorder, $V \neq 0$. Our basic conclusions are as follows: (i) The addition of site disorder breaks the degeneracy between superconducting and charge-density-wave states. Equal-time density-density correlations exhibit a rapid suppression of their staggered pattern, while pair-pair correlations remain robust. (ii) Our data are consistent with an immediate destruction of long-range charge order, while superconducting correlations appear to persist out to a finite $V_c \approx 1.5$. (iii) The behavior of superconducting correlations at $|U|=4$ are in approximate agreement with that of the appropriate magnetic correlations in a strong-coupling model.

An outline of the remainder of this paper is as follows: In Sec. II we give a brief description of the simulation and of the observables used to characterize the ground-state correlations. In Sec. III we present results for local pair and charge correlations. Section IV provides a finite-size scaling analysis of this data to determine the existence of long-range order. We also discuss in some detail the distribution of measurements for different disorder realizations. Section V discusses results for the strong-coupling version of this model, the antiferromagnetic Heisenberg model in a random magnetic field. A summary is presented in Sec. VI.

II. BRIEF DESCRIPTION OF THE SIMULATION

We will use the ‘‘determinant’’ Monte Carlo algorithm²³ for our numerical work. In this approach the partition function is written down as a path integral by discretizing the inverse temperature β , and using the Trotter approximation^{24,25} to break up the exponential of the kinetic and potential pieces of the Hamiltonian. The interaction term is decoupled with a discrete Hubbard-Stratonovich transformation.²⁶ The resulting trace over the fermion operators is over the exponential of quadratic forms, and so it can be done analytically. The result is an expression for the partition function which is the sum over all values of the discrete Hubbard-Stratonovich field of a summand which is the product of two determinants, one each arising from the spin-up and spin-down degrees of freedom. Because both the random site energies and the auxiliary field couple to the charge, the two determinants are identical, and hence their product is positive. There is no fermion sign problem in these simulations, even away from half-filling.

The matrices M_σ , whose determinants give the weight of a particular auxiliary field configuration, are simply related to the equal time fermion Green function: $G_{ij} \equiv \langle c_i c_j^\dagger \rangle = M_{ij}^{-1}$. Observables are measured by expressing them (using Wick’s theorem) in terms of the appropriate sums and products of G . Of particular interest to us here are the equal-time charge and pair correlations,

$$\begin{aligned} c(\mathbf{j}-\mathbf{l}) &= \langle (n_{\uparrow\mathbf{l}} + n_{\downarrow\mathbf{l}} - 1)(n_{\uparrow\mathbf{j}} + n_{\downarrow\mathbf{j}} - 1) \rangle, \\ p_s(\mathbf{j}-\mathbf{l}) &= \langle \Delta_l \Delta_j^\dagger \rangle, \quad \Delta_j^\dagger = c_{\uparrow\mathbf{j}}^\dagger c_{\downarrow\mathbf{j}}^\dagger, \end{aligned} \quad (2)$$

and their associated structure factors

$$S_{\text{cdw}} = \frac{1}{N} \sum_{\mathbf{j}, \mathbf{l}} c(\mathbf{j}-\mathbf{l}) (-1)^{|\mathbf{j}-\mathbf{l}|}, \quad S_{\text{pair}} = \frac{1}{N} \sum_{\mathbf{j}, \mathbf{l}} p_s(\mathbf{j}-\mathbf{l}). \quad (3)$$

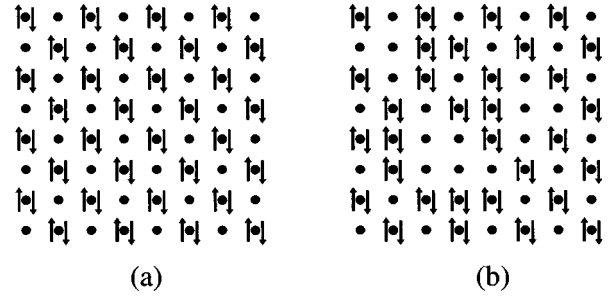


FIG. 1. Two possible real-space configurations of the electrons on the lattice are shown. The pair structure factor attains its largest value $N/4$ for both, while the cdw structure factor is large only for (a).

It is useful to look at a few strong-coupling snapshots of possible real-space electron distributions to gain a preliminary insight into these correlation functions and the effect of site disorder. Consider the strong-coupling limit, when all electrons in the system are paired. A typical low-energy state then consists of a lattice with each site either empty or doubly occupied. A configuration in which the doubly occupied sites alternate with empty sites [Fig. 1(a)] has a lower energy than one in which doubly occupied or empty sites are adjacent by an amount $\Delta E \propto -t^2/U$ to second order in the hopping t . (In the language of the repulsive model onto which the attractive model maps via the particle-hole transformation discussed above, this energy lowering stabilizes antiferromagnetism over ferromagnetism at half-filling, and is proportional to the exchange constant J .) The charge density and pair structure factors defined in Eq. (3) take on their maximal values ($N/4$ for S_{pair} and N for S_{cdw}).

Now consider the effect of site disorder. This will not lead to a breaking of the pairs, but, when the site energies exceed $\propto t^2/U$, it will change the sites on which the pairs prefer to reside [Fig. 1(b)]. Note that the pair structure factor is still large for such a disordered configuration of pairs, since contributions to it depend only on finding doubly occupied sites and empty sites somewhere in the lattice to which to hop. However, the phases in the charge structure factor make it extremely sensitive to the destruction of the original staggered pattern. This rough argument suggests that pair order will be more robust to randomness in the site energy than will charge ordering. Of course, on general grounds we also expect a term in the Hamiltonian which couples directly to the charge to have the greatest effect on the associated charge correlations. Indeed, as discussed by Anderson,²⁷ nonmagnetic impurities are not expected to destroy superconductivity, since one can still pair appropriate eigenstates of the single-particle Hamiltonian which includes the randomness. Even when the disorder is large enough to localize these eigenstates, it has been suggested that superconductivity survives.²⁸

This overview captures the essence of how disorder affects our system. In Sec. III, we will make this qualitative picture more precise.

III. LOCAL CORRELATIONS

We begin by showing some results for the disorder dependence of local quantities. The kinetic energy

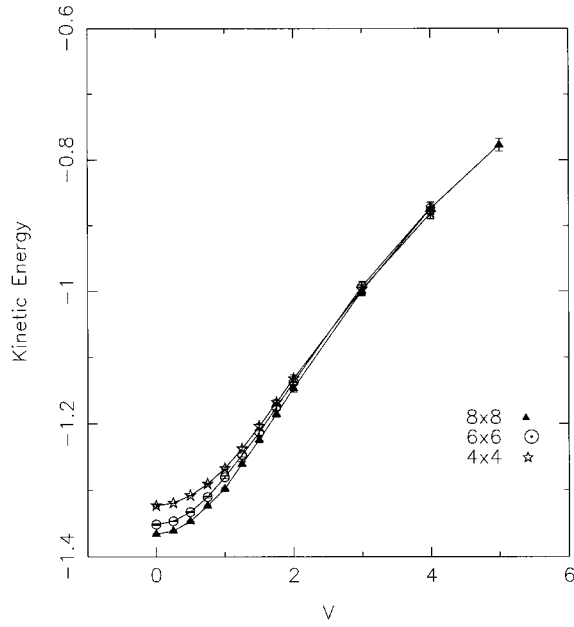


FIG. 2. The kinetic energy as a function of disorder strength.

$\langle k \rangle = -(t/N) \sum_{(i,j)\sigma} (c_{i\sigma}^\dagger c_{j\sigma} + c_{j\sigma}^\dagger c_{i\sigma})$ is shown in Fig. 2. As we shall see below, superconductivity vanishes around $V_c \approx 1.5$. The kinetic energy shows no special signal at this transition. Of course a measure of local electron hopping like $\langle k \rangle$ does not have to vanish at an insulating phase transition.²⁹

In the repulsive Hubbard model, random site energies have a fundamental qualitative effect on the double occupancy rate $\langle n_{j\uparrow} n_{j\downarrow} \rangle$, since they compete with the repulsive interaction and disturb local moment formation. In the attractive model, we expect site disorder to have a much less dramatic effect, and indeed that is seen to be the case in Fig. 3.

Longer range charge-charge correlations are dramatically

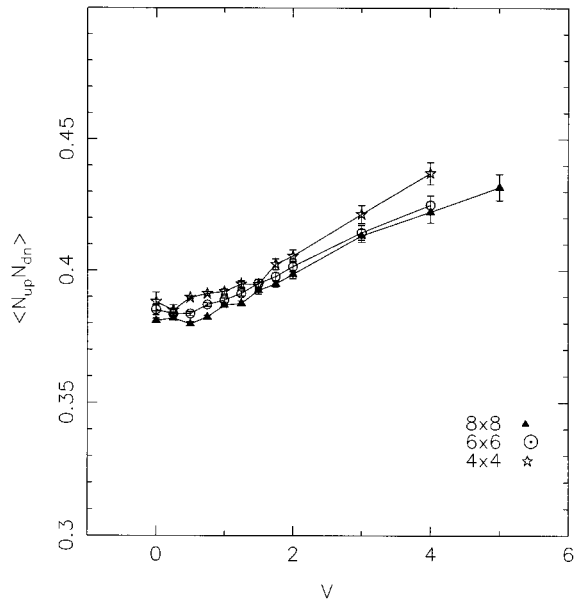


FIG. 3. The double occupancy rate as a function of disorder strength.

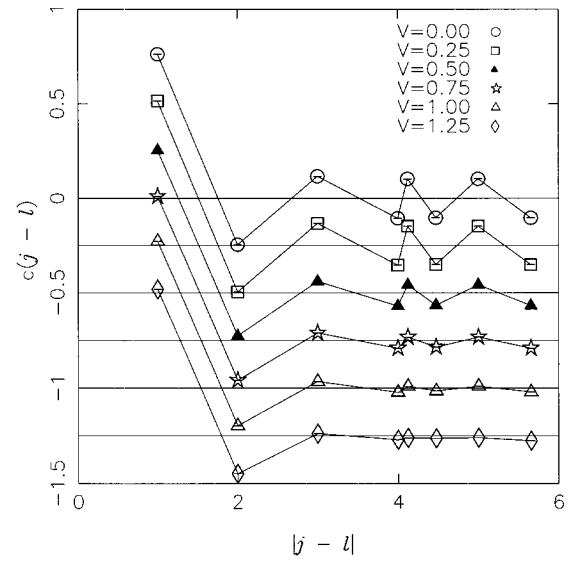


FIG. 4. Charge correlations as a function of site separation for different disorder strengths. Successive disorder strengths have been offset vertically for clarity. The horizontal lines indicate the $c(\mathbf{j}-\mathbf{l})=0$ axis for each successive disorder strength. (The numbers labeling the vertical axis correspond to the $V=0.00$ case.)

affected by site disorder. Figure 4 shows $c(\mathbf{j}-\mathbf{l})$ as a function of lattice separation $\mathbf{j}-\mathbf{l}$ for different disorder strengths. (Successive disorder strengths have been offset vertically for clarity.) The lattice size is 8×8 , inverse temperature $\beta=10$, and $|U|=4$. The oscillatory character of the charge correlations is indicative of cdw ordering. At $V=0$ these correlations extend over the entire lattice; that is, the correlation length ξ exceeds the linear lattice dimension. However as V is turned on the correlations go to zero.

Figure 5 shows the analogous plot for the pair-correlation function $p_s(\mathbf{j}-\mathbf{l})$. The pair correlations remain unchanged for weak V , then are eventually suppressed for sufficiently large randomness. We see the robustness of the pair correla-

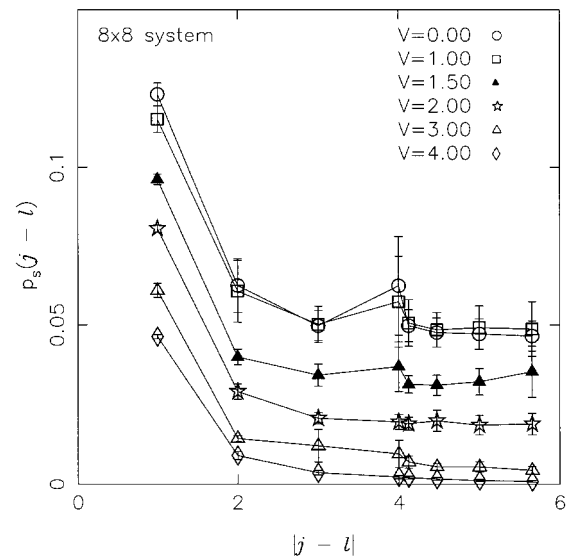


FIG. 5. Pair correlations as a function of site separation for different disorder strengths.

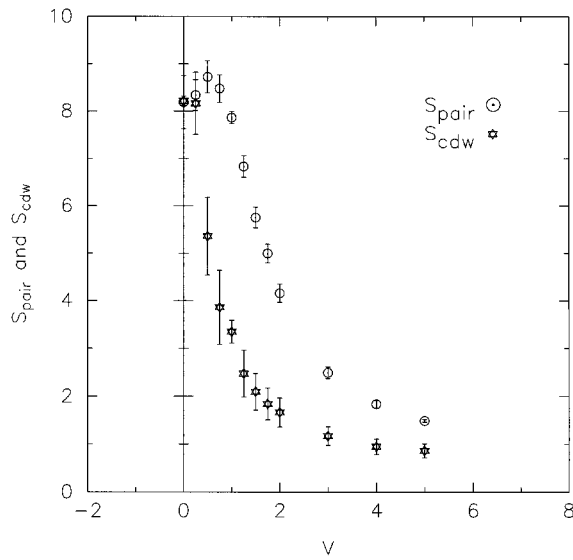


FIG. 6. Charge and pair structure factors as a function of disorder strength.

tions as compared to charge-charge correlations in this plot, which has a much greater range of disorder strengths, V , than does Fig. 4.

The Fourier transforms of these real-space correlation functions are shown as a function of disorder in Fig. 6. The degeneracy between charge and pair correlations is evident in the absence of randomness, $V=0$. As was seen in Figs. 4 and 5, nonzero site disorder more rapidly destroys the charge-density wave than the pair correlations.

IV. DESTRUCTION OF LONG-RANGE ORDER

To determine whether ground-state long-range order exists in our system, we need to do a finite-size scaling analysis. As has been discussed^{30,31} within the context of the repulsive Hubbard model, spin-wave theory³² predicts that on a 2D lattice of size $N=L \times L$, the charge-structure factor and correlation function at largest separation should behave as

$$\frac{1}{N} S_{\text{cdw}} = m^2/3 + a/L, \quad c(L/2, L/2) = m^2/3 + b/L \quad (4)$$

in the ordered phase. Similar results are valid for the pair correlations. Here m is the order parameter. Thus in the ordered phase a plot of the scaled structure factor versus $1/L$ should be a straight line with a nonzero intercept giving $m^2/3$. We will always choose the inverse temperature β sufficiently large that we are effectively at $T=0$ for our finite lattices.

Figure 7 shows the result of this analysis for the charge correlations. The interaction strength is $|U|=4$. Only in the clean system at $V=0$ is a nonzero order parameter m obtained. However, as seen in Fig. 8 the pair field order parameter remains nonzero out to approximately $V=V_c \approx 1.5$.³³

We will conclude this section with a discussion of disorder averaging, since while the other aspects of our simulation are identical to those long reported for determinant Monte Carlo, little is known about what happens when randomness is included. In Fig. 9 we show some histograms of the inter-

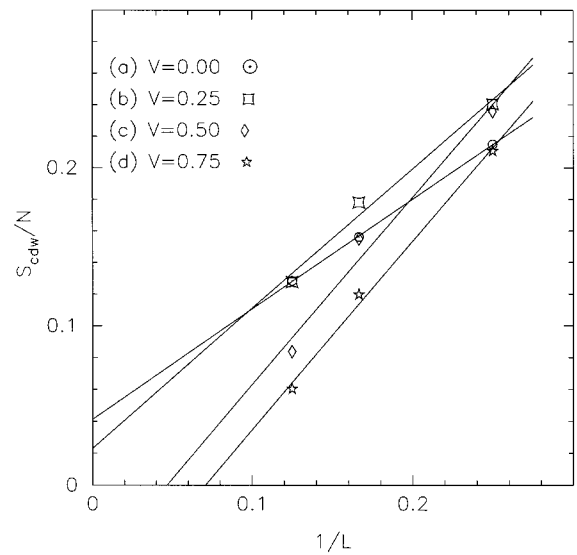


FIG. 7. Finite-size scaling plots for the charge correlations: (a) $V=0.0$, (b) $V=0.25$, (c) $V=0.50$, and (d) $V=0.75$. The straight lines are least-squares fits to the data. Error bars (not shown) on the $V=0.25$ case are consistent with a zero intercept, while error bars on the $V=0.00$ case are not consistent with a zero intercept. The $V=0.00$ (clean case) error bars are much smaller than in the disordered $V=0.25$ case, since there is no disorder averaging required in the clean case.

action and kinetic energies for an 8×8 spatial lattice at an inverse temperature $\beta=10$. We have chosen $|U|=4$ and $V=1$. We see that these quantities have a fairly sharp distribution, that is, the energy is not too sensitive to the detailed disorder realization; the widths of the distributions are less than 5% of the average values. The error bars associated with realization to realization fluctuations in these quantities are roughly ten times the statistical uncertainties in a run consisting of 1000 warm-up sweeps and 5000 measurement sweeps for a single realization.

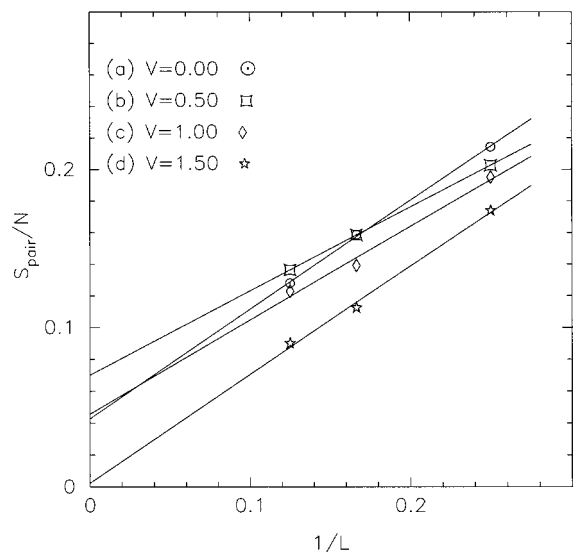


FIG. 8. Finite-size scaling plots for the pair correlations: (a) $V=0.0$, (b) $V=0.50$, (c) $V=1.00$, and (d) $V=1.50$. The straight lines are least-squares fits to the data.

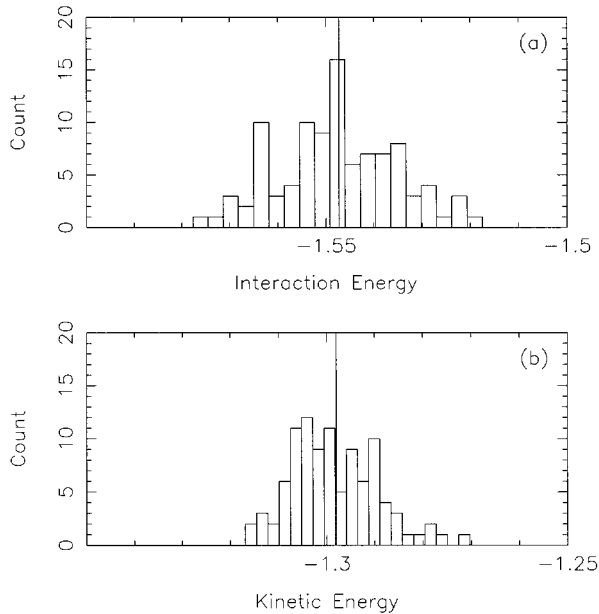


FIG. 9. Histogram of values of the (a) interaction and (b) kinetic energies for different disorder realizations. Each plot represents data from 100 disorder realizations. The average values are shown by the vertical lines.

On the other hand, the fluctuations in quantities which measure long-range correlations are, as expected, much larger. In Fig. 10 we show histograms of the charge and pair structure factors for an 8×8 spatial lattice at inverse temperature $\beta=10$, with $|U|=4$ and $V=1$. We see that the widths of the peaks are of the same order of magnitude as the average values of the respective structure factors.

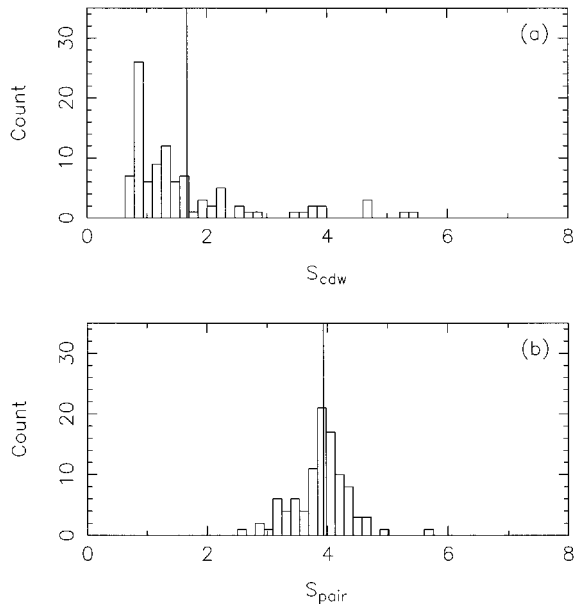


FIG. 10. Histogram of values of the (a) charge and (b) pair structure factors for different disorder realizations. Each plot represents data from 100 disorder realizations. The average values are shown by the vertical lines. The charge structure factor, S_{cdw} , has an apparently non-gaussian form.

We note that practical difficulties limit the number of disorder realizations, and consequently the reduction in fluctuations due to disorder averaging, that one can attain. A single disorder realization for an 8×8 system at $\beta=10$ takes over 1000 CPU minutes on a fast workstation. This computational difficulty of these quantum Monte Carlo calculations precludes disorder averaging over thousands of realizations, as has been done in the spin-glass literature. The non-Gaussian nature of the distributions [e.g., Fig. 10(a)] of course raises difficult questions about how to do the averaging and how to estimate error bars correctly. However, if one goes ahead and employs the usual methods of obtaining error bars based on an assumption of a Gaussian distribution, then averaging over 20–100 disorder realizations reduces the statistical errors to about the same level as the statistical errors associated with the Monte Carlo sampling. This is what we have done in the data reported in this paper.

V. RANDOM-FIELD HEISENBERG MODEL

As we discussed, the attractive ($-U$) Hubbard model can be mapped onto the repulsive model, which in turn at strong coupling can be mapped onto a quantum spin- $\frac{1}{2}$ antiferromagnetic Heisenberg Hamiltonian. In the absence of disorder, the behavior of the associated classical spin models exhibited considerable analogies to the original $-U$ Hubbard model.³ Here we desire to see if similar connections can usefully be made between the disordered $-U$ Hubbard model and the associated classical model—the random field Heisenberg model. However, the problem of the random-field Heisenberg model is an extremely difficult one in its own right. We emphasize that we are attempting only qualitative contact with the attractive Hubbard model simulations here.

We begin by reviewing the results in a uniform magnetic field, since the comparison will be useful in discussing the case of a random field. Similar results were presented in Ref. 3. However, here we present some additional plots which help to characterize more precisely the nature of the ordered phase. In the absence of a field, the continuous symmetry of the model assures us that in 2D there can be no true long range order except in the ground state $T=0$.³⁶ If a field $h_z = \mu$ is applied, the spins tend to lie down in the xy plane, because then they can tilt upwards in the z direction and take advantage of the field energy without costing as much exchange energy J as if they were antiferromagnetically aligned in the z direction. Thus the antiferromagnetic Heisenberg model in a uniform magnetic field is argued to be in the universality class of the XY model, with a finite-temperature Kosterlitz-Thouless phase transition into a state with a power-law decay of the correlation functions. In the language of the attractive model, doping breaks the cdw pair degeneracy, and off half-filling one has a finite-temperature phase transition into a purely superconducting state.⁹

Let us define the antiferromagnetic structure factors in the different spin directions $\alpha = x, y, \text{ and } z$ as the appropriate sums of the correlations of the α component of spin on different sites,

$$S_{\alpha\alpha} = \frac{1}{N} \sum_{\mathbf{j}, \mathbf{l}} \langle s_{\alpha}(\mathbf{j}) s_{\alpha}(\mathbf{l}) \rangle (-1)^{|\mathbf{j}-\mathbf{l}|}. \quad (5)$$

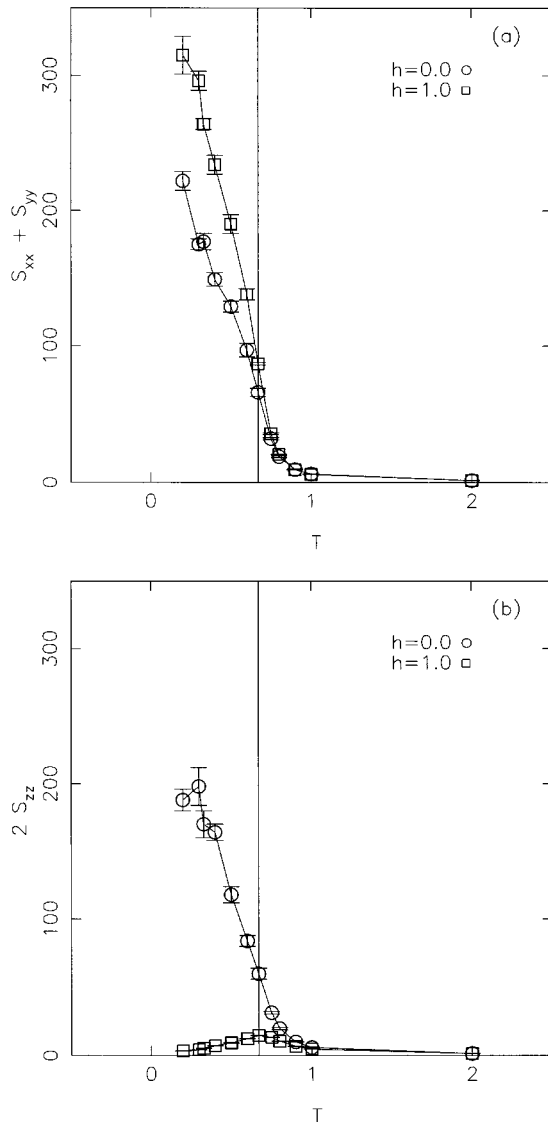


FIG. 11. Results for the structure factors as a function of temperature for a 20×20 lattice. (a) $S_{xx} + S_{yy}$; (b) $2S_{zz}$. The line at $T=0.67$ is at the temperature used in the finite-size scaling plot (Fig. 12) below.

Simulation results for the *classical* antiferromagnetic Heisenberg model in a uniform magnetic field are shown in Figs. 11–13. The temperature dependence is shown first in Fig. 11 on a fixed lattice size. To set a possible scale of T , note that $T_{KT}=0.725$ for the XY model.³⁷ This is consistent with the temperature at which the structure factor swings upward in Fig. 11. We note that a small uniform field, $h_z=1.0$, enhances S_{xx} and S_{yy} substantially, and dramatically reduces S_{zz} . Figure 12 shows the field dependence of the xy structure factors at a fixed $T=0.67$ for different lattices.³⁸ When h_z is nonzero, there is a significant size dependence of the structure factor even at nonzero temperature, which suggests that the presence of a field may indeed make the system order at finite temperature.

Of course these data are only suggestive. A careful finite-size scaling analysis would be needed to pin down whether $T_c=0$ or $T_c \neq 0$. To illustrate one of the issues involved, we note that even if a phase transition occurs only at $T=0$,

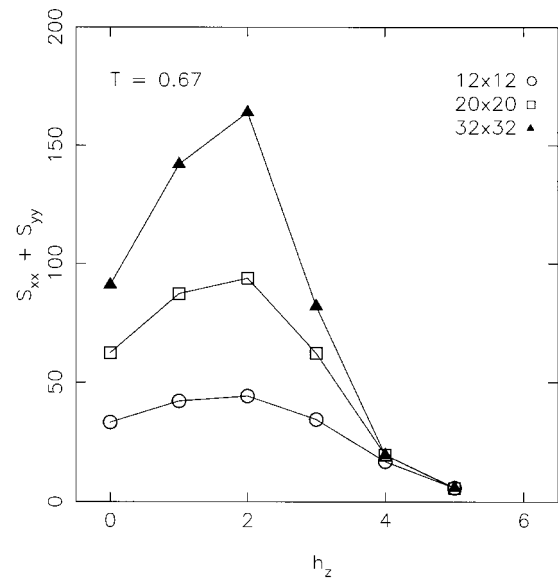


FIG. 12. Results for the xy structure factors as a function of uniform field h_z for different lattice sizes.

structure factors will show significant size dependence up to the lattice size, $L \approx \xi$. In the Heisenberg model, the correlation length $\xi = C_\xi \exp(2\pi J/T)/(1+2\pi J/T)$ where $C_\xi \approx 0.01$.³⁹ Here, with $T=0.67$, the correlation length $\xi \approx 11$. The growth in the structure factors $S_{\alpha\alpha}$ with lattice size at $h_z=0$ is consistent with this value of ξ , and hence with $T_c=0$, as should be the case. The increased growth of $S_{\alpha\alpha}$ with lattice size at nonzero h_z could merely reflect a larger ξ (but T_c still zero) or a finite T_c . The structure factors $S_{\alpha\alpha}$ continue to show the effect of this finite ξ throughout the range of lattice sizes used in the simulations illustrated in Fig. 12. Hence the value of ξ in this model is consistent with the results shown in Fig. 12, being at a temperature where correlations have started to form across the lattice.

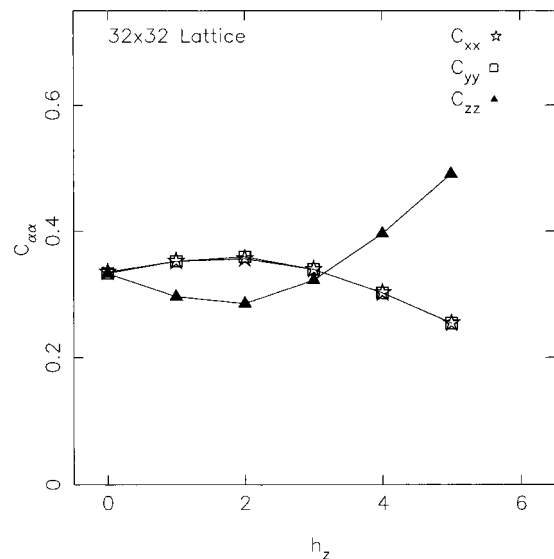


FIG. 13. The averages of the squares of different spin components $C_{\alpha\alpha} = \langle s_\alpha^2 \rangle$ as a function of uniform field h_z . For $h_z=0$ and $C_{xx} = C_{yy} = C_{zz} = \frac{1}{3}$ from rotational invariance.

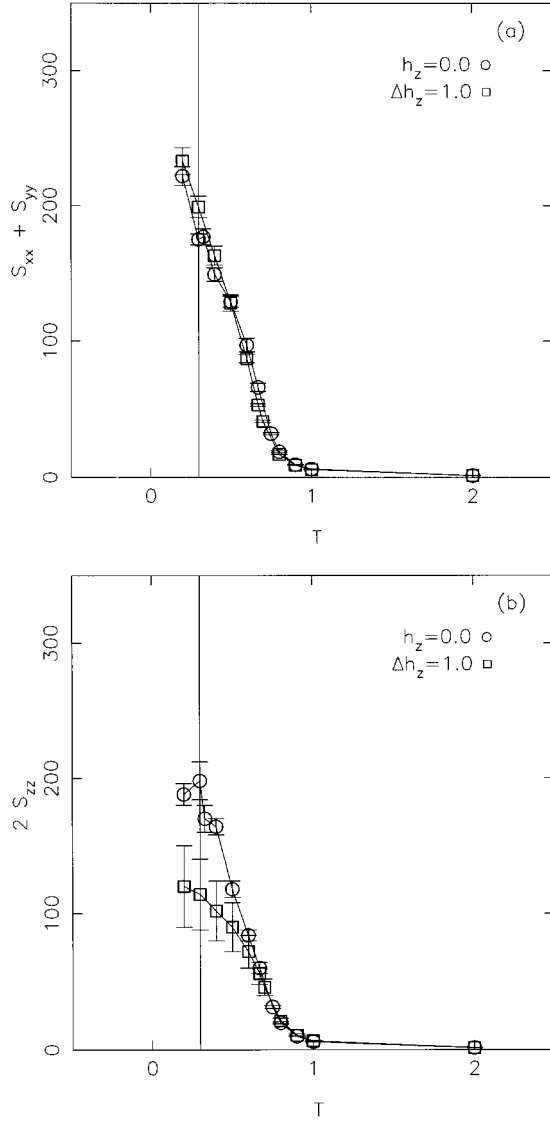


FIG. 14. Results for the structure factors as a function of temperature for a 20×20 lattice in both a zero field ($h_z = 0.0$) and a random field ($\Delta h_z = 1.0$). (a) $S_{xx} + S_{yy}$; (b) $2S_{zz}$. The line at $T = 0.3$ is at the temperature used in the finite-size scaling plots (Fig. 15) below.

We note that while the picture of the spins “lying” down in the xy plane is a physically appealing one, it is not in fact so accurate a view quantitatively. Figure 13 shows the square of the spin components as a function of field strength. We show only one lattice size, 32×32 , since there is no dependence on lattice size for such a local quantity. It is apparent that even for $h_z = 2.0$, where Fig. 12 shows a very significant enhancement of the xy plane structure factor, the spins locally still point almost as much in the z direction as for $h_z = 0.0$. Indeed for larger fields, the spins start to align ferromagnetically with the field, and $\langle s_z^2 \rangle$ exceeds $\langle s_x^2 \rangle = \langle s_y^2 \rangle$. How do we reconcile this with the results for the structure factor? Apparently, the uniform field h_z has a large effect on the long-range spin correlations, and very little effect on the short-range correlations. Thus while individual spins still rotate significantly in the z direction, the antiferromagnetic correlations in the z direction between different spins are de-

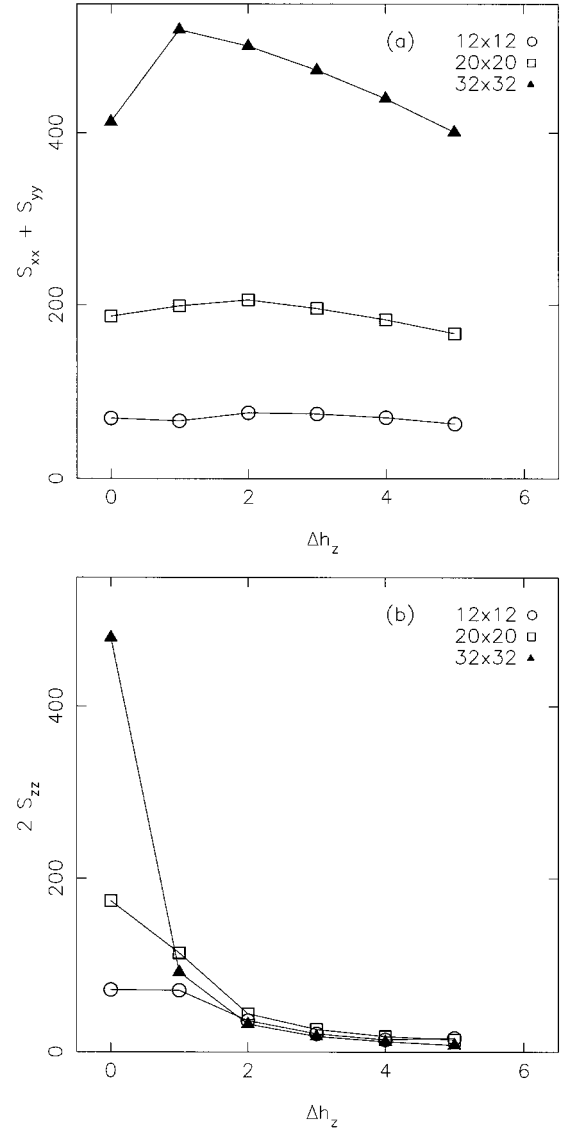


FIG. 15. Results for the structure factors at $T = 0.3$ as a function of random-field strength Δh_z for different lattice sizes. (a) $S_{xx} + S_{yy}$; (b) $2S_{zz}$.

stroyed. (In fact they become ferromagnetic.) At the same time, long-range antiferromagnetic correlations in the plane are enhanced, even though the individual spins are not really “lying down” in the plane.

We now turn to the results of simulations for *random* magnetic fields $h_z(\mathbf{j})$, which is the situation to which our random site energy attractive Hubbard model corresponds. Figures 14 and 15 show analogous plots to those of the uniform field case. Again for low T a random field enhances S_{xx} and S_{yy} , although the effect is much less dramatic than seen in Fig. 11(a). The suppression of S_{zz} is more substantial, but again less decisive than with a uniform field, Fig. 11(b). The random-field results shown in Fig. 15 were obtained at $T = 0.3$, while the results in the corresponding uniform field Fig. 12 were obtained at $T = 0.67$, the temperature at which previously reported uniform-field Heisenberg work was done.³ For intermediate temperatures like $T = 0.67$ it was found that S_{zz} exceeds, by a small amount, S_{xx} and S_{yy} for small disorder. It is not clear to us why this occurs. As seen

by comparing Figs. 11(b) and 14(b), S_{zz} behaves quite differently when the system is subjected to a uniform as opposed to a random field along the z axis. A uniform field suppresses S_{zz} much more strongly than a random field. Nevertheless, in both cases the z -axis structure factor is suppressed with respect to the xy plane structure factors at low enough temperatures.

In Fig. 15, at $T=0.3$, we see that increasing the disorder suppresses the structure factor in the z direction, the analog of the cdw structure factor [Fig. 15(b)], while the structure factors in the xy plane, the analog of the pair structure factor, remain robust to randomness [Fig. 15(a)]. Hence we see the same general results as seen in the disordered, attractive Hubbard model. The analogy is somewhat limited, since we do not see the destruction of the xy plane structure factor [Fig. 15(a)], as disorder is increased, the analog of the destruction of superconductivity (Fig. 6). Determining the critical properties of the random-field Heisenberg model is a problem far beyond the scope of this paper. However, we note that a finite V_c for S_{xx} and S_{yy} is not forbidden, for example, by an Imry-Ma argument, since although the order parameter in this case has continuous symmetry, it is not conjugate to the random disordered h_z field.⁴⁰

We may compare these results with those obtained by Micnas, Robaszkiewicz, and Chao using mean-field theory.⁴¹ The authors mapped the disordered, attractive Hubbard model with nearest-neighbor interactions U_{nn} onto the Heisenberg model in the strong-coupling limit. On-site disorder was drawn either from a uniform distribution or from two δ functions. The finite-temperature phase diagram in the disordered system was found to be particularly rich. In the case $U_{nn}=0$ and with $T=0$, it was found that for a two- δ -function distribution, cdw order is destroyed immediately, but superconducting order persists to a finite V_c . Under the same conditions, but for the uniform site energy distribution used in this paper, the authors found that cdw order is again destroyed immediately but, in contrast to our QMC findings, in MFT no amount of disorder destroys superconductivity.

VI. CONCLUSIONS

We have studied the effect of random site energies on charge-density-wave and superconducting correlations in the

2D attractive Hubbard Hamiltonian at half-filling. We find an immediate suppression of cdw order with a random one-body potential V , whereas the pair order is relatively robust. This is consistent with a strong-coupling picture of the real-space configurations of low-energy states of pairs as disorder is turned on.

After showing the effect of V on the spatial correlations, we performed a finite-size scaling analysis of the structure factors, and determined that a long-range cdw is destroyed for $V_c \approx 0.0$, while superconducting order has $V_c \approx 1.5$, which is roughly the energy scale $4t^2/U \approx 1$ which stabilizes pairing. It is interesting that V_c is considerably less than that required for the destruction of superconductivity in the doped system.²²

We discussed briefly the distribution of different measurements as the disorder configuration was modified. This enabled us to determine a reasonable number of disorder realizations to average over. Finally, the strong-coupling picture of the classical Heisenberg Hamiltonian in a random external field $h_z(\mathbf{j})$ was shown to exhibit some similarities with the disordered attractive Hubbard model results at $|U|=4.0$.

There are a number of further questions we wish to explore. First, we always performed our simulations at an inverse temperature β sufficiently large so that we were in the ground state of the finite size lattices we were studying. The temperature dependence of various quantities would be interesting to determine. We would also like to look more at the non-equal-time, dynamical response of the system. In particular, the issue of how the superconducting gap fills in with disorder is an interesting one. This work requires an analytic continuation of the imaginary-time Green's function, a task which should be challenging, especially in the presence of disorder.

ACKNOWLEDGMENTS

We gratefully acknowledge the help of Mohit Randeria, Nandini Trivedi, and Karl Runge. This work was supported by NSF-DMR-9520776 (R.T.S.), ONR N00014-93-1-0495 (C.H.), and the Associated Western Universities, Inc. (C.H. and R.T.S.). Computer time was provided by the San Diego Supercomputing Center.

¹R. Micnas, J. Ranninger, and S. Robaszkiewicz, Rev. Mod. Phys. **62**, 113 (1990).

²M. Randeria, in *Bose Einstein Condensation*, edited by A. Giffin et al. (Cambridge University Press, Cambridge, 1994).

³R. T. Scalettar, E. Y. Loh, Jr., J. E. Gubernatis, A. Moreo, S. R. White, D. J. Scalapino, R. L. Sugar, and E. Dagotto, Phys. Rev. Lett. **62**, 1407 (1989).

⁴R. M. Fye, M. J. Martins, D. J. Scalapino, J. Wagner, and W. Hanke, Phys. Rev. B **45**, 7311 (1992).

⁵M. Imada, Physica C **185-189**, 1447 (1991).

⁶F. F. Assaad, W. Hanke, and D. J. Scalapino, Phys. Rev. Lett. **71**, 1915 (1993); Phys. Rev. B **49**, 4327 (1994).

⁷F.F. Assaad, R. Preuss, A. Muramatsu, and W. Hanke, J. Low Temp. Phys. **95**, 251 (1994).

⁸Pairing correlations are studied in a three-dimensional attractive Hubbard model in Raimundo R. dos Santos, Phys. Rev. B **50**, 635 (1994). Pairing and cdw correlations on a triangular lattice are discussed in Raimundo R. dos Santos, *ibid.* **48**, 3976 (1993).

⁹A. Moreo and D. J. Scalapino, Phys. Rev. Lett. **66**, 946 (1991).

¹⁰A. Moreo, Phys. Rev. B **45**, 5059 (1992).

¹¹M. Randeria, N. Trivedi, A. Moreo, and R. T. Scalettar, Phys. Rev. Lett. **69**, 2001 (1992).

¹²N. Trivedi and M. Randeria, Phys. Rev. Lett. **75**, 312 (1995).

¹³A. Taraphder, Rahul Pandit, H. R. Krishnamurthy, and T. V. Ra-

- makrishnan, Int. J. Mod. Phys. B **10**, 863 (1996). For theoretical reviews, see P. A. Lee and T. V. Ramakrishnan, Rev. Mod. Phys. **57**, 287 (1985); D. Belitz and T. Kirkpatrick, *ibid.* **66**, 261 (1994).
- ¹⁴D. B. Haviland, Y. Liu, and A. M. Goldman, Phys. Rev. Lett. **62** 2180 (1989); A. F. Hebard and M. A. Paalanen, *ibid.* **65**, 927 (1990); J. M. Valles, R. C. Dynes, and J. P. Garno, *ibid.* **69**, 3567 (1992); A. Yazdani and A. Kapitulnik, *ibid.* **74**, 3037 (1995).
- ¹⁵M. P. A. Fisher, P. B. Weichman, G. Grinstein, and D. S. Fisher, Phys. Rev. B **40**, 546 (1989).
- ¹⁶M. P. A. Fisher, G. Grinstein, and S. M. Girvin, Phys. Rev. Lett. **64**, 587 (1990).
- ¹⁷M. Cha, M. P. A. Fisher, S. M. Girvin, M. Wallin, and A. P. Young, Phys. Rev. B **44**, 6883 (1991).
- ¹⁸E. S. Sorensen, M. Wallin, S. M. Girvin, and A. P. Young, Phys. Rev. Lett. **69**, 828 (1992).
- ¹⁹K. J. Runge, Phys. Rev. B **45**, 13 136 (1992).
- ²⁰G. G. Batrouni, R. T. Scalettar, and G. T. Zimanyi, Phys. Rev. Lett. **65**, 1765 (1990); R. T. Scalettar, G. G. Batrouni, and G. T. Zimanyi, *ibid.* **66**, 3144 (1991); G. G. Batrouni, B. Larson, R. T. Scalettar, J. Tobochnik, and J. Wang, Phys. Rev. B **48**, 9628 (1993).
- ²¹W. Krauth, N. Trivedi, and D. M. Ceperley, Phys. Rev. Lett. **67**, 2307 (1991); M. Makivic, N. Trivedi, and S. Ullah, *ibid.* **71**, 2307 (1993).
- ²²N. Trivedi, R. T. Scalettar, and M. Randeria, Phys. Rev. B **54**, 3756 (1996).
- ²³R. Blankenbecler, R. L. Sugar, and D. J. Scalapino, Phys. Rev. D **24**, 2278 (1981); S. R. White, D. J. Scalapino, R. L. Sugar, E. Y. Loh, Jr., J. E. Gubernatis, and R. T. Scalettar, Phys. Rev. B **40**, 506 (1989).
- ²⁴H. F. Trotter, Proc. Am. Math. Soc. **10**, 545 (1959).
- ²⁵M. Suzuki, Phys. Lett. **113A**, 299 (1985); R. M. Fye, Phys. Rev. B **33**, 6271 (1986).
- ²⁶J. E. Hirsch, Phys. Rev. B **31**, 4403 (1985).
- ²⁷P. W. Anderson, J. Phys. Chem. Solids **11**, 26 (1959).
- ²⁸M. Ma and P. A. Lee, Phys. Rev. B **32**, 5658 (1985).
- ²⁹ $\langle k \rangle = 0$ was used to signal the Mott transition within the Gutzwiller approximation of the fermion Hubbard model, but more recent work has emphasized this is not an appropriate criterion. For results on the behavior of $\langle k \rangle$ at the Mott insulator transition in the boson Hubbard model see G. G. Batrouni, R. T. Scalettar, and G. T. Zimanyi, Phys. Rev. Lett. **65**, 1765 (1990).
- ³⁰J. E. Hirsch and S. Tang, Phys. Rev. Lett. **62**, 591 (1989). The demonstration of long-range order in the large- U , Heisenberg, limit is contained in J. D. Reger and A. P. Young, Phys. Rev. B **37**, 5978 (1988).
- ³¹S. R. White, D. J. Scalapino, R. L. Sugar, E. Y. Loh, J. E. Gubernatis, and R. T. Scalettar, Phys. Rev. B **40**, 506 (1989).
- ³²D. A. Huse, Phys. Rev. B **37**, 2380 (1988).
- ³³Though our error bars do not make possible a definitive statement on this point, it is interesting that there appears a small initial enhancement of the order parameter with V . Similar effects have been seen in the behavior of the staggered magnetization in coupled antiferromagnetic Heisenberg layers, where the order parameter first slightly increases before interplanar coupling drives a paramagnetic phase (Ref. 34). It is also known that T_N can be enhanced by site impurities in the repulsive Hubbard model (Ref. 35).
- ³⁴A. W. Sandvik and D. J. Scalapino, Phys. Rev. Lett. **72**, 2777 (1994).
- ³⁵M. Ulmke, V. Janis, and D. Vollhardt, Phys. Rev. B **51**, 10 411 (1995).
- ³⁶N. D. Mermin and H. Wagner, Phys. Rev. Lett. **17**, 1133 (1966).
- ³⁷D. P. Landau and K. Binder, Phys. Rev. B **24**, 1391 (1981). This reference also shows a phase diagram for the Heisenberg model in a uniform magnetic field. The related, 2D XY planar rotator model, in which the spins are constrained to lie in the xy plane, has a slightly higher T_{KT} of 0.8967(2). See R. Gupta, J. DeLapp, G. G. Batrouni, G. C. Fox, C. F. Baillie, and J. Apostolakis, Phys. Rev. Lett. **61**, 1996 (1988).
- ³⁸These numbers differ from those reported in Ref. 3, for $h_z \approx 3-4$, which were obtained with a Langevin rather than a Monte Carlo simulation. We believe the present values to be correct. In any case, the qualitative results are the same.
- ³⁹S. H. Shenker and J. Tobochnik, Phys. Rev. B **22**, 4462 (1980); P. Kopietz and S. Chakravarty, *ibid.* **40**, 4858 (1989).
- ⁴⁰Y. Imry and S. Ma, Phys. Rev. Lett. **35**, 1399 (1975).
- ⁴¹R. Micnas, S. Robaszkiewicz, and K. A. Chao, Physica A **131**, 393 (1985).